ADVANCED SCIENCE Open Access
www.advancedscience.com

Magnetic Hysteresis at 10 K in Single Molecule Magnet Self-Assembled on Gold

Chia-Hsiang Chen, Lukas Spree, Emmanouil Koutsouflakis, Denis S. Krylov, Fupin Liu, Ariane Brandenburg, Georgios Velkos, Sebastian Schimmel, Stanislav M. Avdoshenko, Alexander Fedorov, Eugen Weschke, Fadi Choueikani, Philippe Ohresser, Jan Dreiser, Bernd Büchner, and Alexey A. Popov**

Tremendous progress in the development of single molecule magnets (SMMs) raises the question of their device integration. On this route, understanding the properties of low-dimensional assemblies of SMMs, in particular in contact with electrodes, is a necessary but difficult step. Here, it is shown that fullerene SMM self-assembled on metal substrate from solution retains magnetic hysteresis up to 10 K. Fullerene-SMM $DySc_2N@C_{80}$ and $Dy_2ScN@C_{80}$ are derivatized to introduce a thioacetate group, which is used to graft SMMs on gold. Magnetic properties of grafted SMMs are studied by X-ray magnetic circular dichroism and compared to the films of nonderivatized fullerenes prepared by sublimation. In self-assembled films, the magnetic moments of the Dy ions are preferentially aligned parallel to the surface, which is different from the disordered orientation of endohedral clusters in nonfunctionalized fullerenes. Whereas chemical derivatization reduces the blocking temperature of magnetization and narrows the hysteresis of $Dy_2ScN@C_{80}$, for $DySc_2N@C_{80}$ equally broad hysteresis is observed as in the fullerene multilayer. Magnetic bistability in the $DySc_2N@C_{80}$ grafted on gold is sustained up to 10 K. This study demonstrates that self-assembly of fullerene-SMM derivatives offers a facile solution-based procedure for the preparation of functional magnetic sub-monolayers with excellent SMM performance.

Since their first discovery in 1993,[1] single molecule magnets (SMMs), i.e., molecular materials with bistable magnetic ground state and slow relaxation of magnetization, have been seen as building elements for nanoscale spintronic devices.[2] Realization of spin valves, giant magnetoresistance, and coherent spin manipulation in single $TbPc_2$ molecules attached to carbon nanotubes at sub-Kelvin temperatures demonstrate the great potential of molecular spintronics with SMMs.[3] A prerequisite for potential nanodevice implementation of a given SMM is that its magnetic bistability demonstrated in bulk powder or crystal sample should be preserved on a substrate, which will serve as an electrode of a device.[4] Thus, surface deposition is a necessary and hardly avoidable step if the truly single-molecule nature of SMMs is to be explored and utilized.[2d,5]

Whereas development of better and stronger SMMs over the last decade was tremendous,[6] the magnetic bistability of SMMs on surfaces is still rather modest in

Prof. C.-H. Chen, Dr. L. Spree, E. Koutsouflakis, Dr. D. S. Krylov, Dr. F. Liu, Dr. A. Brandenburg, G. Velkos, S. Schimmel, Dr. S. M. Avdoshenko, Dr. A. Fedorov, Prof. B. Büchner, Dr. A. A. Popov
Leibniz Institute for Solid State and Materials Research
Helmholtzstraße 20, Dresden 01069, Germany
E-mail: chc@kmu.edu.tw; a.popov@ifw-dresden.de
Prof. C.-H. Chen
Department of Medicinal and Applied Chemistry
Kaohsiung Medical University
Kaohsiung 807, Taiwan

Dr. D. S. Krylov
Center for Quantum Nanoscience
Institute for Basic Science (IBS)
Seoul 03760, Republic of Korea
Dr. A. Fedorov, Dr. E. Weschke
Helmholtz-Zentrum Berlin für Materialien und Energie
Wilhelm-Conrad-Röntgen-Campus BESSY II
Albert-Einstein-Strasse 15, Berlin D-12489, Germany
Dr. F. Choueikani, Dr. P. Ohresser
Synchrotron SOLEIL
L'Orme des Merisiers
Saint-Aubin, BP 48 Gif-sur-Yvette 91192, France
Dr. J. Dreiser
Swiss Light Source
Paul Scherrer Institute
Villigen PSI CH-5232, Switzerland

The ORCID identification number(s) for the author(s) of this article can be found under https://doi.org/10.1002/advs.202000777

DOI: 10.1002/advs.202000777

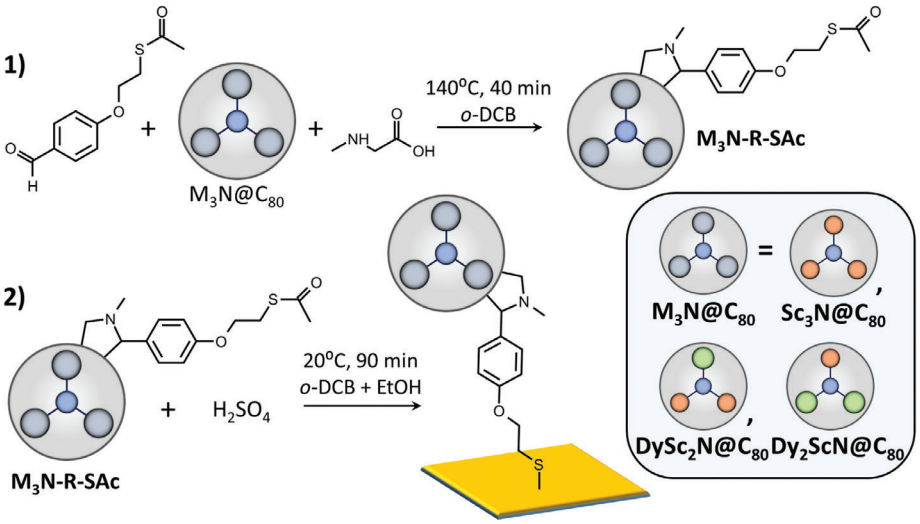

Figure 1. Derivatization of fullerene $M_3N@C_{80}$ with a thioacetate group (M_3N = Sc_3N, $DySc_2N$, and Dy_2ScN) via 1,3-dipolar cycloaddition (1) and deprotection of **M_3N-R-SAc** by acid treatment in *o*-DCB/ethanol leading to the formation of **M_3N-SAM** with partially chemisorbed and partially physisorbed molecules on gold (2).

comparison to bulk SMMs and surface atomic systems. The benchmarks for the sub-monolayers of discrete magnetic units on surfaces are set so far by single atomic magnets such as Ho atoms on MgO|Ag(100) with magnetic bistability up to 30 K.[7] However, processability of single atomic systems outside of an ultrahigh-vacuum chamber is a rather complicated issue. Molecular materials can be processed more easily, and offer chemical routes to surface grafting via solution-based self-assembly. Yet, the studies of the low-dimensional assemblies of SMMs are lagging behind, which is in part caused by the limited stability of many SMM preventing their sublimation and complicating further chemical modification for surface grafting. The best on-surface SMM properties to date have been demonstrated for sublimation-deposited sub-monolayers of $TbPc_2$ with magnetic bistability up to 8–9 K on MgO|Ag(100)[8] and graphene/SiC(0001)[9] substrates.

Fullerenes as carbon cages with empty voids capable of storing magnetic clusters offer important advantages on this route.[10] On the one hand, the magnetism of endohedral species can be tuned in a broad range by judicious choice of encapsulated metals and their combinations.[11] On the other hand, the carbon cage is very stable thermally and chemically, which enables sublimation[12] or further chemical functionalization[13] of endohedral metallofullerenes (EMFs). In this work we use these advantages to prepare self-assembled sub-monolayer films (SAMs) of fullerenes $DySc_2N@C_{80}$ and $Dy_2ScN@C_{80}$ on Au(111) and achieve the highest temperature of magnetic hysteresis for SMMs on a metallic substrate.

Due to the close distance to the central nitride ion, Dy ions in both EMFs have strong magnetic anisotropy. The two molecules are different only in the number of Dy ions in the endohedral trimetal cluster, which however has a strong influence on their low-temperature SMM behavior. $DySc_2N@C_{80}$ shows quantum tunneling of magnetization (QTM) near zero field and has a blocking temperature of magnetization (T_B) near 7 K,[14] whereas intramolecular dipolar and exchange interactions between Dy ions in $Dy_2ScN@C_{80}$ quench the QTM and shift the T_B to 8 K.[15]

To graft these EMFs to gold substrates, they were first functionalized with a thioacetate (SAc) linker via 1,3-dipolar cycloaddition (**Figure 1**) using a modification of the procedure described earlier for C_{60}.[16] In the original procedure in ref. [16], C_{60} was functionalized with a thiol linker. However, EMFs require higher reaction temperature, and direct thiol attachment to EMFs was found unstable, requiring the use of a more stable thioacetate linker instead. Cycloaddition reactions were performed for three $M_3N@C_{80}$ molecules (M_3N = Sc_3N, $DySc_2N$, and Dy_2ScN) giving pure derivatives (denoted as **M_3N-RSAc** hereafter) after chromatographic separation. Further details and characterization of the products are given in ESI (Figures S1–S7, Supporting Information).

SQUID (superconducting quantum interference device) magnetometry proved that the fullerenes retained their SMM behavior after derivatization. **$DySc_2$N-RSAc** has similarly broad hysteresis as the pristine $DySc_2N@C_{80}$, whereas its T_B is increased to 8 K (Figure S7, Supporting Information). For $Dy_2ScN@C_{80}$ the cycloaddition resulted in a narrower hysteresis and a reduced T_B of 4 K in **Dy_2ScN-RSAc** (Figure S8, Supporting Information). These findings agree well with the earlier results on fullerene cycloadducts.[17] The different influence of cycloaddition on the hysteretic behavior of $DySc_2N@C_{80}$ and $Dy_2ScN@C_{80}$ is not very clear. Presumably, the main reason is the different mechanism of the magnetization relaxation in two SMMs at low temperature. Whereas in-field relaxation of magnetization in single-on magnet $DySc_2N@C_{80}$ is governed by the Raman mechanism,[14a] in $Dy_2ScN@C_{80}$ the relaxation follows the Orbach mechanism via the state with antiferromagnetic coupling of Dy moments.[15b] The latter process may be more susceptible to the changes of vibrational density of states in the molecules when the internal motion of the cluster is hindered by the cycloadduct.

The previous attempt of obtaining EMF-SMM monolayers with thioether linker –S–CH_3 in a similar molecular arrangement resulted in a low coverage of physisorbed molecules.[17a] In this work, chemisorption (Figure 1) was attempted following

ref. [18] by dissolving **M_3N-RSAc** derivatives in *o*-dichlorobenzene (DCB)/ethanol (10:1) and adding H_2SO_4 in the presence of Au(111)/mica substrates (PHASIS, Switzerland). After incubation in solution for 90 min, the substrates were washed with an excess of *o*-DCB followed by ethanol and dried in a flow of nitrogen. Formation of self-assembled films with sub-monolayer coverage (**M_3N-SAMs** hereafter) was verified by XPS (X-ray photoelectron spectroscopy; Figure S9, Supporting Information) and X-ray absorption spectroscopy (XAS, see below). XPS spectra in the S 2p range revealed the presence of Au-bonded sulfur at 161.1 eV, nonbonded sulfur at 162–163 eV and a broad signal of oxidized sulfur at 169 eV (Figure S9, Supporting Information). The oxidized sulfur likely originates form the traces of the sulfuric acid used in the deposition procedure, which is in line with the higher sulfur content than expected for the chemical composition of the functionalized fullerenes. Considering that Au-bonded and nonbonded sulfur originates from chemi- and physisorbed molecules, the former constitute ≈40% in **$DySc_2$N-SAM** and 30% in **Dy_2ScN-SAM**. The SAMs prepared from C_{60} functionalized with thioacetate groups by Tour et al.[18a] exhibited similar XPS spectra with bonded and nonbonded sulfur. Since ellipsometry analysis proved formation of monolayers in their samples, the authors concluded that functionalized C_{60} molecules may pack in a head-to-tail manner on the surface. This contamination precluded complete monolayer coverage of the metal surface with fullerenes, thus giving sub-monolayer films as a result of solution-based self-assembly. XAS analysis of our samples (see below) also excludes formation of multilayers, and we thus conclude that our sub-monolayer **M_3N-SAMs** consist of a mixture of chemi- and physisorbed molecules, for which head-to-tail arrangement may be a reasonable possibility.

Structural and magnetic properties of the SAMs were then studied by X-ray natural linear dichroism (XNLD) and X-ray magnetic circular dichroism (XMCD) at the Dy-$M_{4,5}$ absorption edge. For each sample, we first discuss the XNLD and XMCD spectra and their angular dependence to establish possible ordering of fullerene molecules on the surface, and then proceed to the description of the hysteretic behavior. As a reference, XAS measurements were also performed for the films of nonfunctionalized fullerenes on Au(111) prepared by vacuum evaporation.

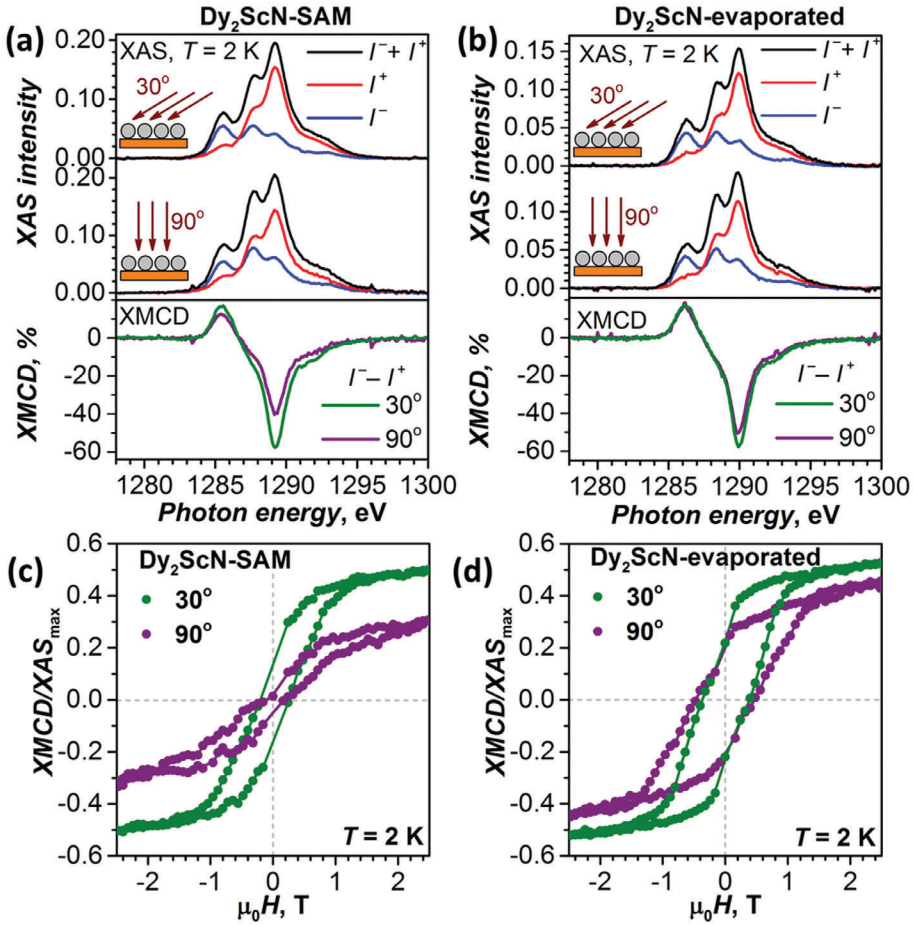

Figure 2. XAS and XMCD spectra of Dy_2ScN-SAM a) and evaporated Dy_2ScN@C_{80} sub-monolayer b) on Au(111) measured at 30° and 90° orientation of the X-ray and magnetic field versus the surface; $T \approx 2$ K, $H = 6.5$ T, only the Dy-M_5 edge is shown (see the Supporting Information for the whole Dy-$M_{4,5}$ range). X-ray polarizations are denoted at I^+ and I^-, nonpolarized XAS is a sum of I^+ and I^-, and XMCD is their difference normalized to the maximum of XAS. Magnetic hysteresis of Dy_2ScN-SAM c) and evaporated Dy_2ScN@C_{80} sub-monolayer d) on Au(111) measured by XMCD technique for two orientations of the sample; $T \approx 2$ K, sweep rate 2 T min^{-1}; dots are experimental values, lines are added to guide the eye. The measurements of the evaporated sub-monolayer are from ref. [22].

XAS studies of **Dy_2ScN-SAM** were performed at the UE46_PGM-1 beamline[19] at BESSY II (Helmholtz-Zentrum Berlin) and the X-Treme beamline at the Swiss Light Source (Paul Scherrer Institute).[20] XNLD and XMCD experiments at two beamlines with fresh **Dy_2ScN-SAM** samples prepared immediately before the measurements demonstrated good reproducibility of the procedure (Figure S10, Supporting Information). Total XAS intensity of **Dy_2ScN-SAM** is only slightly higher than that of the evaporated sub-monolayer with ca 0.5 monolayer coverage (**Figure 2**a,b; Figures S11 and S12, Supporting Information), proving that the deposition procedure did not form multilayers and is limited to a sub-monolayer coverage. At room temperature, a Dy-M_5 XNLD signal of 13% of the XAS maximum was observed indicating partial ordering of the Dy_2ScN clusters in the SAM (Figure S10, Supporting Information; see also Figure S13 (Supporting Information) for simulations of XAS and XNLD spectra with the code MULTIX[21]). Low temperature XMCD measurements at 2–5 K also confirmed this observation. Figure 2a shows XAS and XMCD spectra at the Dy-M_5 edge in two orientations of the beam and magnetic field versus the surface. The XMCD signal at grazing incidence (30°) is noticeably stronger than for the normal incidence (90°) indicating that the magnetic moments of Dy^{3+} ions tend to be parallel to the surface. Importantly, the ordering effect in the **Dy_2ScN-SAM** is more pronounced that in the sub-monolayer of nonfunctionalized $Dy_2ScN@C_{80}$ (Figure 2b, see also Figures S14–S16 (Supporting Information) and ref. [22] for more details). Note also that earlier we could not observe ordering for thioether-functionalized $Dy_2ScN@C_{80}$ physisorbed on Au(111).[17a,23] Thus, cycloaddition to the fullerene cage freezes rotation of the endohedral cluster inside the fullerene, whereas the self-assembly hinders rotation of the molecules on the surface. Angular dependence of magnetization is also evident from magnetic hysteresis measurements (Figure 2c). At 2 K, **Dy_2ScN-SAM** demonstrates magnetic hysteresis at both incidence angles of 30° and 90°. In line with the SQUID measurements of powder samples (Figure S8, Supporting Information), the opening of the hysteresis for **Dy_2ScN-SAM** is narrower than for the sub-monolayer of $Dy_2ScN@C_{80}$ (Figure 2d).

Because of the considerable remanence and coercivity found in its powder samples,[15] $Dy_2ScN@C_{80}$ was in focus of the earlier surface studies of EMF-SMMs, and magnetic properties of its

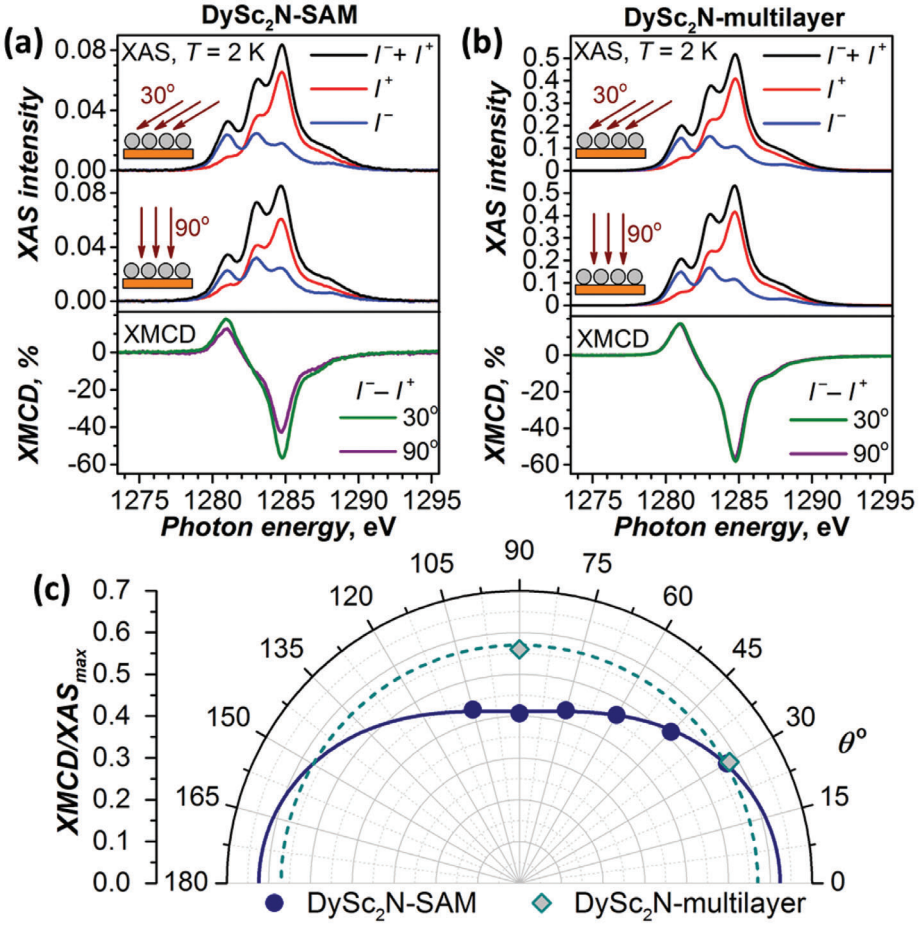

Figure 3. XAS and XMCD spectra of $DySc_2N$-SAM a) and evaporated $DySc_2N@C_{80}$ multilayer b) on Au(111) measured at 30° and 90° orientations of the X-ray and magnetic field versus the surface; $T \approx 2$ K, $H = 6$ T, only the Dy-M_5 edge is shown (see the Supporting Information for the whole Dy-$M_{4,5}$ range). c) Angular dependence of XMCD asymmetry for $DySc_2N$-SAM on Au(111). θ is defined as the angle between X-ray beam/magnetic field and the surface, dots are experimental values, solid line is a fit with the function $XMCD/XAS = C_1\cos^2(\theta) + C_2$. Dashed line shows the isotopic distribution for a completely disordered cluster ($C_1 = 0$) such as found for the $DySc_2N@C_{80}$ multilayer.

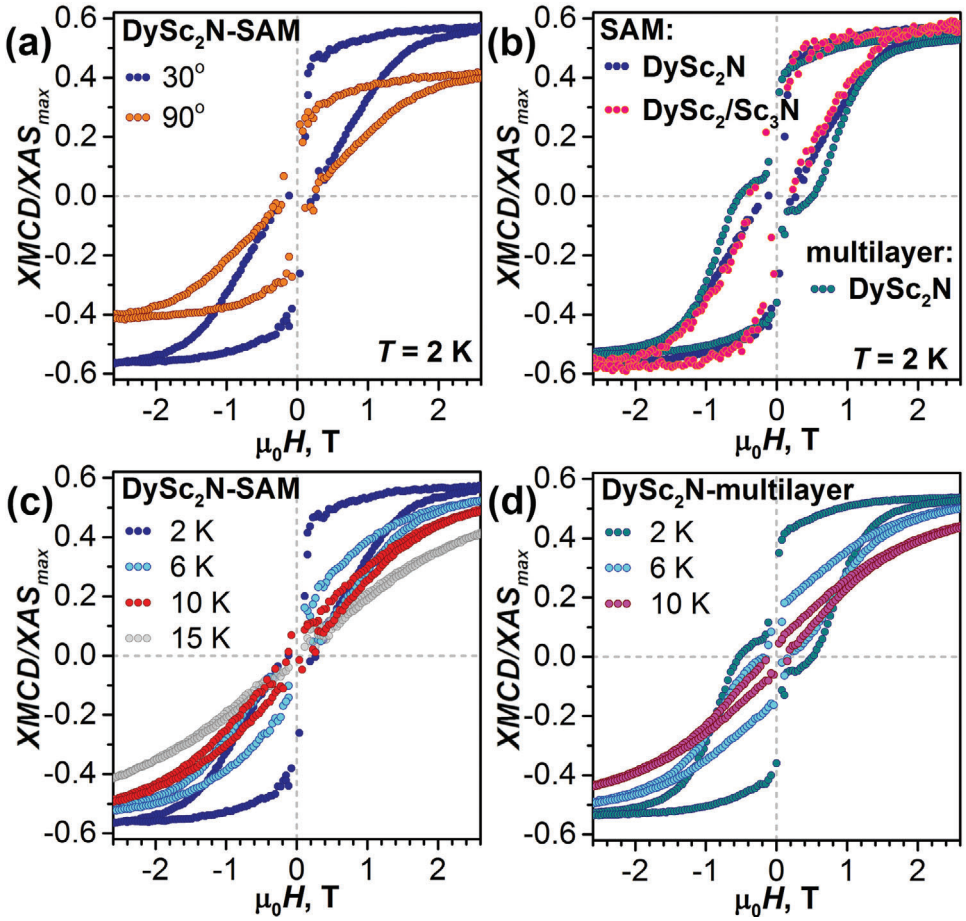

Figure 4. Magnetic hysteresis curves measured by XMCD technique, sweep rate 2 T min^{-1}. a) $DySc_2N$-SAM measured at 30° and 90°; $T \approx 2$ K; b) $DySc_2N$-SAM, diluted $DySc_2/Sc_3N$-SAM, and $DySc_2N@C_{80}$ multilayer measured at 30°, $T \approx 2$ K. c) $DySc_2N$-SAM measured at 30° at different temperatures; d) $DySc_2N@C_{80}$ multilayer on Au(111) measured at 30° at different temperatures.

monolayers were studied by XMCD on Rh(111), *h*-BN|Rh(111), Au(111), Ag(100), and MgO(10 ML)|Ag(100).[12] All of them exhibited magnetic hysteresis near 2 K, but none retained magnetic bistability at 6 K. Meanwhile, it appears that the magnetism of the dinuclear Dy_2ScN cluster is more susceptible to the external effects than that of the mononuclear $DySc_2N$. As described above, exohedral functionalization of the fullerene decreases the temperature range of magnetic bistability of $Dy_2ScN@C_{80}$, but improves the SMM behavior of $DySc_2N@C_{80}$.[17a] Likewise, $DySc_2N@C_{80}$ retains magnetic hysteresis inside carbon nanotubes, whereas the $Dy_2ScN@C_{80}$-based peapod does not show magnetic hysteresis.[24] Below we demonstrate that SMM behavior of a $DySc_2N@C_{80}$ monolayer on a metallic substrate is also more robust than that of $Dy_2ScN@C_{80}$.

XAS and XMCD studies of **$DySc_2N$-SAM** were performed at the DEIMOS beamline at synchrotron SOLEIL.[25] In agreement with the molecular composition, XAS intensity of **$DySc_2N$-SAM** is twice smaller than that of **Dy_2ScN-SAM** (**Figure 3**), which also proves similar sub-monolayer coverage of the gold surface by fullerene molecules in both SAMs. At room temperature **$DySc_2N$-SAM** showed XNLD signal with the relative intensity of 7%, which increased to 8% upon lowering temperature to 2 K (Figure S17, Supporting Information). A noticeable angular dependence can be also seen in the XMCD spectra measured between 30° and 90° (Figure 3; Figure S18, Supporting Information). The XMCD signal increases gradually with the decrease of the incidence angle from 90° to 30° (Figure 3c), showing that the orientation of the $DySc_2N$ cluster parallel to the surface is more preferable.

As a reference, a multilayer film (5–6 monolayers) of non-functionalized $DySc_2N@C_{80}$ was prepared by evaporation onto an Au(111) single crystal. For such a film, XMCD does not show any angular dependence (Figure 3; Figure S19, Supporting Information), proving that the endohedral cluster is completely disordered, although carbon cages form ordered closed-packed hexagonal layers as can be seen in the STM topography (Figures S20 and S21, Supporting Information).

Figure 4a shows that at 2 K **$DySc_2N$-SAM** has an open magnetic hysteresis between −2 T and 2 T. Near zero field the hysteresis tends to close due to the fast relaxation of magnetization via QTM as also observed in the bulk powder sample (Figure S7, Supporting Information). Hysteresis of a $DySc_2N@C_{80}$ multilayer at 2 K is similarly broad, but demonstrates noticeable deviations from **$DySc_2N$-SAM** in the field less than 1 T (Figure 4b). Note that due to the peculiarities of the total electron yield detection mode, the XMCD intensity during the field sweep shows

erratic oscillations at small magnetic fields, which prevents an accurate measurement of the hysteresis shape close to 0 T. Very recent sub-Kelvin study of $\{Fe_4\}$ molecular magnet deposited on superconducting Pb(111) surface showed that this problem can be mitigated by very low sweep rate and continuous switching of the X-ray beam polarity,[26] and the use of this approach seems promising in future studies of QTM in EMF monolayers.

The QTM of $DySc_2N@C_{80}$ strongly depends on the molecular environment and can be reduced significantly by magnetic dilution.[14a,17b] To find if moderate dilution can have a similar effect on surface, a SAM was prepared from a 1:4 mixture of **$DySc_2N$-RSAc** and **Sc_3N-RSAc**. Dy-$M_{4,5}$ XAS intensity of **$DySc_2$/Sc_3N-SAM** is decreased according to the four-fold dilution (Figures S22 and S23, Supporting Information), but the shape of the hysteresis remains virtually identical to that of **$DySc_2N$-SAM** (Figure 4b). Unfortunately, studies of a stronger on-surface dilution are limited by a decreasing signal-to-noise ratio.

Magnetization curves of **$DySc_2N$-SAM** and $DySc_2N@C_{80}$ multilayer were then measured at different temperatures. Figure 4c demonstrates that the hysteresis in **$DySc_2N$-SAM** is getting narrower with the temperature increase, but still remains open at 10 K (see also Figure S24 in the Supporting Information for more temperatures). Thus, the surface grafting is not deteriorating SMM properties of the $DySc_2N@C_{80}$ derivative. However, a direct comparison of the monolayer XMCD studies to the results of SQUID magnetometry for powder samples may appear not fully representative because of the X-ray demagnetization effect[27] and other differences in the measurement conditions, such as the magnetic field sweep rate. A bulletproof evidence is provided by the comparison between **$DySc_2N$-SAM** and $DySc_2N@C_{80}$ multilayer, representing the properties of the bulk fullerene material. Similar hysteretic behavior found by XMCD for the two samples (compare Figure 4c,d) proves that the direct contact with the metallic substrate does not affect the magnetic bistability of $DySc_2N@C_{80}$ in the SAM. This is different from $TbPc_2$ on Au(111), which exhibits open hysteresis up to 15 K in a multilayer, but shows no hysteresis in the monolayer at 8 K.[28]

To conclude, we have functionalized metallofullerene-SMMs $DySc_2N@C_{80}$ and $Dy_2ScN@C_{80}$ with surface-anchoring groups and prepared self-assembled sub-monolayer films thereof on Au(111) from solution. Chemical functionalization is found to influence the SMM properties of both fullerenes, and appears to be beneficial for $DySc_2N@C_{80}$, which increases the blocking temperature of magnetization in the cycloadduct. Most importantly, XMCD studies of SAMs revealed that the metallic substrate does not impose a considerable influence on the SMM behavior of surface-grafted fullerenes, which is attributed to the shielding of magnetic units by the carbon cage. This allows the self-assembled sub-monolayer of the $DySc_2N@C_{80}$ derivative to exhibit the highest temperature of hysteresis yet observed in SMM monolayers on surfaces proving its high potential for the exploration of SMM-based spintronic devices. In the future, further optimization of the deposition procedure may be required to maximize the ratio of chemisorbed molecules.

Supporting Information

Supporting Information is available from the Wiley Online Library or from the author.

Acknowledgements

The authors acknowledge funding from the European Union's Horizon 2020 Research and Innovation Programme, European Research Council (Grant Agreement No. 648295 to A.A.P.). J.D. acknowledges funding by the Swiss National Science Foundation (Grant No. 200021_165774/1). The authors appreciate the help in SQUID measurements by Dr. Anja Wolter-Giraud and Sebastian Gaß, and Marco Rosenkranz for NMR characterization. The authors are grateful to the SOLEIL, Swiss Light Source, and BESSY II staff for smoothly running the facilities. This work was funded by LabEx PALM (ANR-10-LABX-0039-PALM). XPS measurements were performed at Russian–German beamline at BESSY II.[29]

Conflict of Interest

The authors declare no conflict of interest.

Keywords

fullerenes, magnetic hysteresis, self-assembled monolayers, single-molecule magnets, XMCD

Received: March 2, 2020
Revised: November 26, 2020
Published online: January 21, 2021

[1] R. Sessoli, D. Gatteschi, A. Caneschi, M. A. Novak, *Nature* **1993**, *365*, 141.

[2] a) C. Cervetti, E. Heintze, L. Bogani, *Dalton Trans.* **2014**, *43*, 4220; b) L. Bogani, W. Wernesdorfer, *Nat. Mater.* **2008**, *7*, 179. c) G. Cucinotta, L. Poggini, A. Pedrini, F. Bertani, N. Cristiani, M. Torelli, P. Graziosi, I. Cimatti, B. Cortigiani, E. Otero, P. Ohresser, P. Sainctavit, A. Dediu, E. Dalcanale, R. Sessoli, M. Mannini, *Adv. Funct. Mater.* **2017**, *27*, 1703600; d) K. Katoh, T. Komeda, M. Yamashita, *Chem. Rec.* **2016**, *16*, 987; e) A. Cornia, P. Seneor, *Nat. Mater.* **2017**, *16*, 505; f) A. Gaita-Ariño, F. Luis, S. Hill, E. Coronado, *Nat. Chem.* **2019**, *11*, 301.

[3] a) E. Moreno-Pineda, C. Godfrin, F. Balestro, W. Wernsdorfer, M. Ruben, *Chem. Soc. Rev.* **2018**, *47*, 501; b) C. Godfrin, A. Ferhat, R. Ballou, S. Klyatskaya, M. Ruben, W. Wernsdorfer, F. Balestro, *Phys. Rev. Lett.* **2017**, *119*, 187702; c) I. V. Krainov, J. Klier, A. P. Dmitriev, S. Klyatskaya, M. Ruben, W. Wernsdorfer, I. V. Gornyi, *ACS Nano* **2017**, *11*, 6868; d) M. Urdampilleta, S. Klayatskaya, M. Ruben, W. Wernsdorfer, *ACS Nano* **2015**, *9*, 4458; e) M. Ganzhorn, S. Klyatskaya, M. Ruben, W. Wernsdorfer, *Nat. Nanotechnol.* **2013**, *8*, 165; f) R. Vincent, S. Klyatskaya, M. Ruben, W. Wernsdorfer, F. Balestro, *Nature* **2012**, *488*, 357; g) M. Urdampilleta, S. Klyatskaya, J. P. Cleuziou, M. Ruben, W. Wernsdorfer, *Nat. Mater.* **2011**, *10*, 502.

[4] a) M. Mannini, F. Pineider, C. Danieli, F. Totti, L. Sorace, P. Sainctavit, M. A. Arrio, E. Otero, L. Joly, J. C. Cezar, A. Cornia, R. Sessoli, *Nature* **2010**, *468*, 417; b) M. Mannini, F. Pineider, P. Sainctavit, C. Danieli, E. Otero, C. Sciancalepore, A. M. Talarico, M.-A. Arrio, A. Cornia, D. Gatteschi, R. Sessoli, *Nat. Mater.* **2009**, *8*, 194.

[5] a) A. Cornia, M. Mannini, P. Sainctavit, R. Sessoli, *Chem. Soc. Rev.* **2011**, *40*, 3076; b) N. Domingo, E. Bellido, D. Ruiz-Molina, *Chem. Soc. Rev.* **2012**, *41*, 258; c) R. J. Holmberg, M. Murugesu, *J. Mater. Chem. C* **2015**, *3*, 11986; d) E. Moreno Pineda, T. Komeda, K. Katoh, M. Yamashita, M. Ruben, *Dalton Trans.* **2016**, *45*, 18417; e) C. Carbone, S. Gardonio, P. Moras, S. Lounis, M. Heide, G. Bihlmayer, N. Atodiresei, P. H. Dederichs, S. Blügel, S. Vlaic, A. Lehnert, S. Ouazi, S. Rusponi, H. Brune, J. Honolka, A. Enders, K. Kern, S. Stepanow, C. Krull, T. Balashov, A. Mugarza, P. Gambardella, *Adv. Funct. Mater.* **2011**, *21*, 1212; f) A. Cornia, D. R. Talham, M. Affronte, in *Molecular*

Magnetic Materials (Eds: B. Sieklucka, D. Pinkowicz), Wiley-VCH, New York **2017**, p. 187.

[6] a) J.-L. Liu, Y.-C. Chen, M.-L. Tong, *Chem. Soc. Rev.* **2018**, *47*, 2431; b) K. L. M. Harriman, D. Errulat, M. Murugesu, *Trends Chem* **2019**, *1*, 425; c) C. A. P. Goodwin, F. Ortu, D. Reta, N. F. Chilton, D. P. Mills, *Nature* **2017**, *548*, 439; d) F.-S. Guo, B. M. Day, Y.-C. Chen, M.-L. Tong, A. Mansikkamäki, R. A. Layfield, *Science* **2018**, *362*, 1400.

[7] F. Donati, S. Rusponi, S. Stepanow, C. Wäckerlin, A. Singha, L. Persichetti, R. Baltic, K. Diller, F. Patthey, E. Fernandes, J. Dreiser, Ž. Šljivančanin, K. Kummer, C. Nistor, P. Gambardella, H. Brune, *Science* **2016**, *352*, 318.

[8] C. Wäckerlin, F. Donati, A. Singha, R. Baltic, S. Rusponi, K. Diller, F. Patthey, M. Pivetta, Y. Lan, S. Klyatskaya, M. Ruben, H. Brune, J. Dreiser, *Adv. Mater.* **2016**, *28*, 5195.

[9] G. Serrano, E. Velez-Fort, I. Cimatti, B. Cortigiani, L. Malavolti, D. Betto, A. Ouerghi, N. B. Brookes, M. Mannini, R. Sessoli, *Nanoscale* **2018**, *10*, 2715.

[10] a) A. A. Popov, *Endohedral Fullerenes: Electron Transfer and Spin*, Springer International Publishing, Cham, Switzerland **2017**; b) T. Wang, C. Wang, *Small* **2019**, *15*, 1901522.

[11] a) L. Spree, A. A. Popov, *Dalton Trans.* **2019**, *48*, 2861; b) F. Liu, L. Spree, D. S. Krylov, G. Velkos, S. M. Avdoshenko, A. A. Popov, *Acc. Chem. Res.* **2019**, *52*, 2981.

[12] a) T. Greber, A. P. Seitsonen, A. Hemmi, J. Dreiser, R. Stania, F. Matsui, M. Muntwiler, A. A. Popov, R. Westerström, *Phys. Rev. Mater.* **2019**, *3*, 014409; b) R. Westerström, A.-C. Uldry, R. Stania, J. Dreiser, C. Piamonteze, M. Muntwiler, F. Matsui, S. Rusponi, H. Brune, S. Yang, A. Popov, B. Büchner, B. Delley, T. Greber, *Phys. Rev. Lett.* **2015**, *114*, 087201.

[13] a) P. Jin, Y. Li, S. Magagula, Z. Chen, *Coord. Chem. Rev.* **2019**, *388*, 406; b) L. Bao, P. Peng, X. Lu, *Acc. Chem. Res.* **2018**, *51*, 810; c) M. d. C. Gimenez-Lopez, J. A. Gardener, A. Q. Shaw, A. Iwasiewicz-Wabnig, K. Porfyrakis, C. Balmer, G. Dantelle, M. Hadjipanayi, A. Crossley, N. R. Champness, M. R. Castell, G. A. D. Briggs, A. N. Khlobystov, *Phys. Chem. Chem. Phys.* **2010**, *12*, 123.

[14] a) D. Krylov, F. Liu, A. Brandenburg, L. Spree, V. Bon, S. Kaskel, A. Wolter, B. Buchner, S. Avdoshenko, A. A. Popov, *Phys. Chem. Chem. Phys.* **2018**, *20*, 11656; b) R. Westerström, J. Dreiser, C. Piamonteze, M. Muntwiler, S. Weyeneth, H. Brune, S. Rusponi, F. Nolting, A. Popov, S. Yang, L. Dunsch, T. Greber, *J. Am. Chem. Soc.* **2012**, *134*, 9840.

[15] a) D. S. Krylov, F. Liu, S. M. Avdoshenko, L. Spree, B. Weise, A. Waske, A. U. B. Wolter, B. Büchner, A. A. Popov, *Chem. Commun.* **2017**, *53*, 7901; b) R. Westerström, J. Dreiser, C. Piamonteze, M. Muntwiler, S. Weyeneth, K. Krämer, S.-X. Liu, S. Decurtins, A. Popov, S. Yang, L. Dunsch, T. Greber, *Phys. Rev. B* **2014**, *89*, 060406.

[16] M. del Carmen Gimenez-Lopez, M. T. Räisänen, T. W. Chamberlain, U. Weber, M. Lebedeva, G. A. Rance, G. A. D. Briggs, D. Pettifor, V. Burlakov, M. Buck, A. N. Khlobystov, *Langmuir* **2011**, *27*, 10977.

[17] a) C. H. Chen, D. S. Krylov, S. M. Avdoshenko, F. Liu, L. Spree, R. Westerström, C. Bulbucan, M. Studniarek, J. Dreiser, A. U. B. Wolter, B. Büchner, A. A. Popov, *Nanoscale* **2018**, *10*, 11287; b) Y. Li, T. Wang, H. Meng, C. Zhao, M. Nie, L. Jiang, C. Wang, *Dalton Trans.* **2016**, *45*, 19226.

[18] a) Y. Shirai, L. Cheng, B. Chen, J. M. Tour, *J. Am. Chem. Soc.* **2006**, *128*, 13479; b) N. Crivillers, Y. Takano, Y. Matsumoto, J. Casado-Montenegro, M. Mas-Torrent, C. Rovira, T. Akasaka, J. Veciana, *Chem. Commun.* **2013**, *49*, 8145.

[19] E. Weschke, E. Schierle, *J. Large-Scale Res. Facil.* **2018**, *4*, A127.

[20] C. Piamonteze, U. Flechsig, S. Rusponi, J. Dreiser, J. Heidler, M. Schmidt, R. Wetter, M. Calvi, T. Schmidt, H. Pruchova, J. Krempasky, C. Quitmann, H. Brune, F. Nolting, *J. Synchrotron Radiat.* **2012**, *19*, 661.

[21] A. Uldry, F. Vernay, B. Delley, *Phys. Rev. B* **2012**, *85*, 125133.

[22] D. S. Krylov, S. Schimmel, V. Dubrovin, F. Liu, T. T. N. Nguyen, L. Spree, C.-H. Chen, G. Velkos, C. Bulbucan, R. Westerström, M. Studniarek, J. Dreiser, C. Hess, B. Büchner, S. M. Avdoshenko, A. A. Popov, *Angew. Chem., Int. Ed.* **2020**, *59*, 5756.

[23] S. M. Avdoshenko, *J. Comput. Chem.* **2018**, *39*, 1594.

[24] a) R. Nakanishi, J. Satoh, K. Katoh, H. Zhang, B. K. Breedlove, M. Nishijima, Y. Nakanishi, H. Omachi, H. Shinohara, M. Yamashita, *J. Am. Chem. Soc.* **2018**, *140*, 10955; b) S. Avdoshenko, F. Fritz, C. Schlesier, A. Kostanyan, J. Dreiser, M. Luysberg, A. A. Popov, C. Meyer, R. Westerström, *Nanoscale* **2018**, *10*, 18153.

[25] P. Ohresser, E. Otero, F. Choueikani, K. Chen, S. Stanescu, F. Deschamps, T. Moreno, F. Polack, B. Lagarde, J.-P. Daguerre, F. Marteau, F. Scheurer, L. Joly, J.-P. Kappler, B. Muller, O. Bunau, P. Sainctavit, *Rev. Sci. Instrum.* **2014**, *85*, 013106.

[26] G. Serrano, L. Poggini, M. Briganti, A. L. Sorrentino, G. Cucinotta, L. Malavolti, B. Cortigiani, E. Otero, P. Sainctavit, S. Loth, F. Parenti, A.-L. Barra, A. Vindigni, A. Cornia, F. Totti, M. Mannini, R. Sessoli, *Nat. Mater.* **2020**, *19*, 546.

[27] J. Dreiser, R. Westerström, C. Piamonteze, F. Nolting, S. Rusponi, H. Brune, S. Yang, A. Popov, L. Dunsch, T. Greber, *Appl. Phys. Lett.* **2014**, *105*, 032411.

[28] L. Margheriti, D. Chiappe, M. Mannini, P. E. Car, P. Sainctavit, M.-A. Arrio, F. B. de Mongeot, J. C. Cezar, F. M. Piras, A. Magnani, E. Otero, A. Caneschi, R. Sessoli, *Adv. Mater.* **2010**, *22*, 5488.

[29] S. I. Fedoseenko, I. E. Iossifov, S. A. Gorovikov, J. S. Schmidt, R. Follath, S. L. Molodtsov, V. K. Adamchuk, G. Kaindl, *Nucl. Instrum. Methods Phys. Res., Sect. A* **2001**, *470*, 84.

